Energy Bands for V_3X Compounds

L. F. MATTHEISS
Bell Telephone Laboratories, Murray Hill, New Jersey
(Received 31 August 1964; revised manuscript received 30 November 1964)

The augmented-plane-wave (APW) method has been used to calculate energy bands for a number of V_3X compounds having the β-wolfram structure, including hypothetical V_3Al, V_3Si, V_3Co, V_3Ga, V_3Ge, and V_3As. These calculations have been carried out at symmetry points in the Brillouin zone for all the above compounds and, in addition, along symmetry lines for V_3Ga so that a rough density of states could be constructed for this compound. It has been found that: (a) the calculated density of states is in qualitative agreement with the schematic model proposed by Clogston and Jaccarino to explain the temperature dependence of the Knight shifts and the susceptibility for V_3Ga; (b) the Fermi energy for V_3Ga coincides with a peak in the density-of-states curve which is due primarily to the vanadium $3d$ bands; (c) the APW wave functions at the Fermi surface for V_3Ga contain an admixture of gallium $4p$ character which is an order of magnitude smaller than that predicted by Clogston and Jaccarino to account for the negative Knight shift at the gallium site; (d) to a good approximation, a rigid-band model can be used to represent the variation in the density of states at the Fermi surface for the series of compounds V_3Ga, V_3Ge, and V_3As; (e) the energy bands for hypothetical V_3Al and V_3Si are very similar to those obtained for V_3Ga and V_3Ge, respectively; (f) the gross features of the energy bands for these compounds are relatively insensitive to the potentials used in these calculations, though the width and position of the vanadium $3d$ bands relative to the other pertinent bands is potential-dependent; (g) the linear chain model for these V_3X compounds provides an inadequate description of their energy-band structure.

I. INTRODUCTION

THE binary intermetallic compounds having the A_3B composition and the β-wolfram structure are of some theoretical interest and practical importance because they include materials with the highest superconducting transition temperatures that have been observed to date. Matthias, Geballe, and Compton[1] have tabulated the forty-odd compounds with this structure that have been prepared thus far and this information is summarized in Table I. In this table the compounds are divided according to the atomic number of the B atom; for those compounds which have been found to become superconducting, the transition temperatures are given in parentheses. According to Table I, the A atom is always a transition element, while the B atoms can be either transition or nontransition elements. From an energy-band point of view, it is reasonable to divide these A_3B compounds into two categories, depending on whether the B atom is a transition or nontransition element. If gold is included with the transition elements, then those compounds in the first four columns of Table I fall into one category while those in the last three fall into the other.

Some of the interesting electronic properties which these compounds possess, in addition to their high-superconducting transition temperatures, have been summarized previously by Clogston and Jaccarino.[2] These properties include:

(a) A large low-temperature electronic specific heat for V_3Si and V_3Ga[3];

(b) strongly temperature-dependent Knight shifts and susceptibilities for those compounds with high superconducting transition temperatures[4,5];

(c) positive vanadium atom Knight shifts which decrease with decreasing temperature;

(d) negative B atom Knight shifts, the magnitudes of which increase with decreasing temperature;

(e) susceptibilities which increase with decreasing temperatures.

To explain these experimental results, Clogston and Jaccarino[2] have proposed a rather schematic energy-band model for V_3Ga. They assume a conduction band formed principally from vanadium $4s$ and $4p$ and gallium $4p$-type atomic states which overlaps a narrower band formed mainly from the vanadium $3d$-type states. The gallium $4s$ electrons are assumed to occupy a band far below the Fermi energy. The Fermi energy for V_3Ga is assumed to coincide with a peak in the density-of-states curve which is due primarily to vanadium $3d$- and gallium $4p$-type atomic states. From the temperature dependence of the susceptibility, they estimate that this peak has a characteristic width of approximately 0.04 eV. The negative Knight shift at the gallium sites is attributed to core polarization by the gallium $4p$ electrons at the Fermi surface. At the vanadium sites, the positive Knight shift is explained in terms of a combined temperature-independent orbital paramagnetism[6] and temperature-dependent core polarization by vanadium $3d$ electrons at the Fermi surface.

In order to determine the validity for this model, the augmented-plane-wave (APW) method[7] has been

[1] B. T. Matthias, T. H. Geballe, and V. B. Compton, Rev. Mod. Phys. **35**, 1 (1963).
[2] A. M. Clogston and V. Jaccarino, Phys. Rev. **121**, 1357 (1961).
[3] F. J. Morin and J. P. Maita, Phys. Rev. **129**, 1115 (1963).
[4] W. E. Blumberg, J. Eisinger, V. Jaccarino, and B. T. Matthias, Phys. Rev. Letters **5**, 149 (1960).
[5] H. J. Williams and R. C. Sherwood, Bull. Am. Phys. Soc. Ser. II, **5**, 430 (1960).
[6] A. M. Clogston, A. C. Gossard, V. Jaccarino, and Y. Yafet, Phys. Rev. Letters **9**, 262 (1962).
[7] J. C. Slater, Phys. Rev. **51**, 846 (1937).

TABLE I. Summary of the A_3B compounds having the β-wolfram structure, divided according to the atomic number of the B atom. The superconducting transition temperatures are given in parentheses in those cases where they have been measured.

					13 Al	14 Si	15 P
					Nb_3Al(17.5) Mo_3Al(0.58)	V_3Si(17.1) Cr_3Si Mo_3Si(1.30)	
26 Fe	27 Co	28 Ni	29 Cu	30 Zn	31 Ga	32 Ge	33 As
	V_3Co				V_3Ga(16.5) Cr_3Ga Nb_3Ga(14.5) Mo_3Ga(0.76)	V_3Ge(6.01) Cr_3Ge Nb_3Ge(6.90) Mo_3Ge(1.43)	V_3As
44 Ru	45 Rh	46 Pd	47 Ag	48 Cd	49 In	50 Sn	51 Sb
Cr_3Ru(3.3)	V_3Rh(0.38) Cr_3Rh Nb_3Rh(2.50)				Nb_3In(9.2)	V_3Sn(7.0) Nb_3Sn(18.05) Ta_3Sn(6.4)	Ti_3Sb(5.8) V_3Sb(0.80) Nb_3Sb
76 Os	77 Ir	78 Pt	79 Au	80 Hg	81 Tl	82 Pb	83 Bi
Nb_3Os(1.05) Mo_3Os(7.2)	Ti_3Ir(5.4) V_3Ir Cr_3Ir(0.45) Nb_3Ir(1.7) Mo_3Ir(8.8)	Ti_3Pt(0.58) V_3Pt(2.83) Cr_3Pt Nb_3Pt(9.2)	Ti_3Au V_3Au(0.74) Zr_3Au(0.92) Nb_3Au(11.5)			Zr_3Pb(0.76)	

used to calculate energy bands for several V_3X compounds having the β-wolfram structure, where X=Al, Si, Co, Ga, Ge, and As. (Hereafter, V_3X will be used to designate those A_3B compounds with vanadium atoms at the A sites.) The basic APW computer programs, originally written by Saffren[8] and Wood[9] for monatomic crystal structures, have been extended by Switendick[10] to handle structures containing two different types of atoms per unit cell. Only minor modifications to Switendick's general program were required to handle the β-wolfram structure.

The results of the APW calculations for V_3Ga agree qualitatively with the schematic density-of-states model proposed by Clogston and Jaccarino. A pair of bands which are predominantly gallium 4s-like in character are found to lie well below the Fermi energy, separated by an energy gap from the overlapping conduction bands. The vanadium 3d bands are found to have a width of approximately 0.5 Ry and lie in the midst of bands which represent the vanadium 4s-, 4p-, and gallium 4p-type states. These vanadium 3d bands exhibit considerable anisotropy and are divided roughly into two sub-bands, separated by a minimum in the density of states, similar to that found by Wood[9] for body-centered cubic iron. The gross features of these 3d bands are fairly insensitive to the potentials used in these calculations as well as to the particular atom at the X site, and are qualitatively similar for V_3Ga, V_3Ge, V_3As, and hypothetical V_3Al and V_3Si.

The calculated density of states for V_3Ga exhibits considerable structure in addition to the minimum described above. There is a peak in the density of states just before this minimum, and the Fermi energy for V_3Ga falls at this peak. Assuming a rigid-band model, the Fermi energy for V_3Ge falls near the leading edge of this peak, while that for V_3As lies near the minimum in the density-of-states curve.

Analysis of the APW wave functions for V_3Ga in the vicinity of the Fermi energy suggests that they are predominantly vanadium 3d-like in character, the admixture of gallium 4p character being less than 5%. Clogston and Jaccarino have estimated that approximately equal amounts of vanadium 3d and gallium 4p character are required at the Fermi surface to account for the temperature-dependent Knight shifts at the respective sites. Limited studies indicate that the admixture of gallium 4p character at the Fermi surface is not enhanced appreciably by reasonable variations in the vanadium or gallium potentials used in the present series of calculations.

The most striking feature of these V_3X compounds is the high density of states at the Fermi energy $N(0)$ which is inferred from the low-temperature electronic specific heat and susceptibility measurements. In the case of V_3Ga, the specific heat and susceptibility measurements yield values for $N(0)$ of 7.1 and 5.6 spin states per eV-vanadium atom, respectively. The latter result is only approximate since it is obtained by correcting the measured susceptibility for orbital effects, as estimated by Clogston *et al.*[6] These values for $N(0)$ are two or three times larger than those found in transition metals. They are several times larger than the value of 1.3 spin states per eV-vanadium atom which results from a crude density-of-states calculation for V_3Ga, based on the present APW results. This situation has led Clogston[11] to suggest that the sus-

[8] M. M. Saffren, Bull. Am. Phys. Soc. **5**, 298 (1960).
[9] J. H. Wood, Phys. Rev. **126**, 517 (1962).
[10] A. C. Switendick, Solid-State and Molecular Theory Group, Massachusetts Institute of Technology, Quarterly Progress Report No. 49, p. 41, 1963 (unpublished).
[11] A. M. Clogston, Phys. Rev. **136**, A8 (1964).

ceptibilities and specific heats for these V_3X compounds are strongly affected by exchange and electron-phonon interactions, respectively. Using reasonable estimates for these interaction parameters, Clogston has shown that the effect of such interactions is to exaggerate the temperature dependence of the susceptibility and to enhance the low-temperature specific heat. As a result of this proposal, a less severe peak in the density of states at the Fermi surface is required to interpret the specific heat and susceptibility data for V_3Ga.

Recently, Weger[12] has proposed an energy-band model for V_3Ga and V_3Si which emphasizes the one-dimensional chains of atoms which exist in the β-wolfram structure. He points out that the nearest-neighbor vanadium distance, d is somewhat smaller than the distance between vanadium atoms belonging to different chains, $(\frac{3}{2})^{1/2}d$. Using a tight-binding approximation and considering only nearest-neighbor interactions, he finds $3d$ energy bands and a Fermi surface which reflect these one-dimensional properties. A similar analysis, carried through during the present investigation, indicates that this linear chain model predicts an oversimplified $3d$ energy band structure for these V_3X compounds.

A detailed discussion of the symmetry properties of the β-wolfram structure is contained in the following section. This section also includes a description of the APW method as it is applied to these compounds and a discussion of the methods used to calculate the potentials used in the present series of calculations. Section III contains the results of these APW calculations, an analysis of the wave functions in various energy ranges, and a description of the density-of-states calculation. The linear chain model for the β-wolfram compounds is treated in Sec. IV. The last section contains a general discussion of the APW results and their relation to experiment.

II. DESCRIPTION OF THE CALCULATION

The space group for the A_3B compounds having the β-wolfram structure is $O_h^3(Pm3n)$, which is a nonsymmorphic space group with a simple cubic Bravais lattice. The distribution of atoms in the simple cubic unit cell is shown in Fig. 1, where the A atoms are represented touching spheres and the B atoms are shaded. The B atoms occupy body-centered cubic positions while the A atoms are situated on the faces of the simple cube. The point-group symmetries at the B and A atom sites are $T_h(m3)$ and $D_{2h}(\bar{4}2m)$, respectively.

The nearest neighbors to an A atom are two other A atoms at a distance of $\frac{1}{2}a$, where a is the cube edge. These atoms form chains parallel to the coordinate axes. The second neighbors to an A atom are four B atoms, at a distance $\frac{1}{4}\sqrt{5}a$, while the third neighbors are eight A atoms at a distance $\frac{1}{4}\sqrt{6}a$. These third neighbor atoms belong to chains perpendicular to the chain containing the atom at the origin. The nearest neighbors to a B atom are twelve A atoms at a distance $\frac{1}{4}\sqrt{5}a$, which indicates the close-packed nature of this structure.

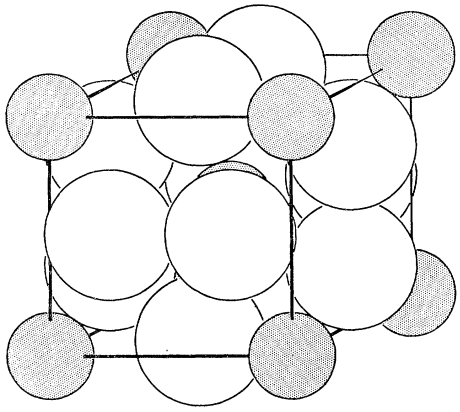

FIG. 1. Distribution of atoms in the unit cell for the A_3B compounds having the β-wolfram structure. The A atoms are represented by touching spheres on the surface of the simple-cubic unit cell while the B-atom spheres occupy body-centered cubic positions. These B-atom spheres are shaded and are not drawn with maximum radii.

The unit cell for the β-wolfram structure contains six A and two B atoms, so that one expects a large number of valence electrons per unit cell and a correspondingly large number of occupied energy bands below the Fermi energy. For example, in V_3Ga, the gallium $3d$ bands are occupied and well below the energy range of the $4s$-$4p$ bands. Since each vanadium atom has five electrons in the $3d$-$4s$ atomic states, we expect 30 electrons per unit cell in the corresponding energy-band states. Similarly, each gallium atom contributes two $4s$ and one $4p$ electrons for a total of six electrons per unit cell. This yields a total of 36 electrons per unit cell for V_3Ga, so that the Fermi surface must fall somewhere in the vicinity of the 18th band, assuming each band is doubly occupied by electrons of either spin. The situation for V_3Al, V_3Si, V_3Ge, and V_3As is analogous. In the case of V_3Co, each cobalt atom contributes the nine electrons associated with the $3d$-$4s$ atomic states, yielding a total of 48 electrons per unit cell.

The symmetry properties for the space group O_h^3 have been investigated independently by Gorzkowski[13] and the present author.[14] Although the irreducible representations for this space group are available in the literature, we shall summarize these results here for convenience. As usual, the irreducible representations for points inside the first Brillouin zone can be obtained rather simply from those for the corresponding point group. On the surface of the Brillouin zone, the

[12] M. Weger, Rev. Mod. Phys. **36**, 175 (1964).

[13] W. Gorzkowski, Phys. Stat. Solidi **3**, 910 (1963).

[14] L. F. Mattheiss, Solid-State and Molecular Theory Group, Massachusetts Institute of Technology, Quarterly Progress Report No. 51, p. 54, 1964 (unpublished).

irreducible representations can be different. The Brillouin zone for the simple cubic lattice is shown in Fig. 2, where the notation of Bouckaert, Smoluchowski, and Wigner[15] is used to label symmetry points and lines. The point group of the wave vector at the symmetry points X and M on the surface of the Brillouin zone is D_{4h}, with sixteen operations. At X, four two-dimensional irreducible representations are found, while at M, there are eight one-dimensional (M_i, $i=1, 8$) and two two-dimensional (M_9 and M_{10}) irreducible representations. At the point R, the point group of the wave vector is O_h, and there are three two-dimensional representations (R_1, R_2, and R_3) and one six-dimensional representation (R_4). Gorzkowski has pointed out that R_1 and R_2 are degenerate as a consequence of time reversal symmetry. Along the symmetry line T, the point group of the wave vector is C_{4v}, with eight operations. Along this line, there are four one-dimensional (T_1, T_2, T_3, and T_4) and one two-dimensional (T_5) irreducible representations. The point group of the wave vector along the lines S and Z is C_{2v}, with four operations. Along S, there is one two-dimensional representation while Z has four one-dimensional representations. The relation between the notation established by Bouckaert, Smoluchowski, and Wigner and that used by Gorzkowski for points inside the first Brillouin zone and along the line Z is given in Table II. The compatibility relations for points on the surface

TABLE II. Relation between the notation of Gorzkowski (G) and Bouckaert, Smoluchowski, and Wigner (BSW) for points inside the first Brillouin zone and along the line Z.

BSW	G	BSW	G	BSW	G
Γ_1	Γ_1^+	Δ_1	Δ_1	Λ_1	Λ_1
$\Gamma_{1'}$	Γ_1^-	Δ_2	Δ_2	Λ_2	Λ_2
Γ_2	Γ_2^+	Δ_2'	Δ_3	Λ_3	Λ_3
$\Gamma_{2'}$	Γ_2^-	Δ_1'	Δ_4		
Γ_{12}	Γ_3^+	Δ_5	Δ_5	Z_1	Z_1
$\Gamma_{12'}$	Γ_3^-			Z_4	Z_2
$\Gamma_{15'}$	Γ_4^+	Σ_1	Σ_1	Z_2	Z_3
Γ_{15}	Γ_4^-	Σ_4	Σ_2	Z_3	Z_4
$\Gamma_{25'}$	Γ_5^+	Σ_2	Σ_3		
Γ_{25}	Γ_5^-	Σ_3	Σ_4		

of the Brillouin zone are summarized in Table III. In this latter table and in the following discussions, the notation used is identical to that introduced by Gorzkowski, except in those instances where he deviates from the more standard notation of Bouckaert, Smoluchowski, and Wigner.

The energy bands in the free-electron approximation have been computed for the β-wolfram structure and are shown in Fig. 3. In the V_3X compounds, although the vanadium $3d$ bands alter the distribution of states drastically in the vicinity of the Fermi energy, these results are useful when one attempts to identify the origin of the calculated states. This identification

[15] L. P. Bouckaert, R. Smoluchowski, and E. Wigner, Phys. Rev. **50**, 58 (1936).

TABLE III. Compatibility relations for points on the surface of the Brillouin zone.

X_1		X_2		X_3			X_4		
S_1		S_1		S_1			S_1		
Z_1Z_3		Z_2Z_4		Z_3Z_4			Z_1Z_2		
$\Delta_1\Delta_2$		$\Delta_{1'}\Delta_{2'}$		Δ_5			Δ_5		
R_1		R_2		R_3			R_4		
S_1		S_1		S_1			$3S_1$		
T_5		T_5		T_5			$T_1T_2T_3T_4T_5$		
Λ_3		Λ_3		Λ_3			$\Lambda_1\Lambda_2 2\Lambda_3$		
M_1	M_2	M_3	M_4	M_5	M_6	M_7	M_8	M_9	M_{10}
Σ_4	Σ_4	Σ_2	Σ_2	Σ_2	Σ_1	Σ_3	Σ_3	$\Sigma_1\Sigma_4$	$\Sigma_2\Sigma_3$
Z_3	Z_1	Z_2	Z_4	Z_3	Z_1	Z_2	Z_4	Z_1Z_3	Z_2Z_4
T_2	T_1	T_2	T_1	T_4	T_3	T_4	T_3	T_5	T_5

of states is considerably more difficult in the β-wolfram structure than it is in the case of the transition metals, for example. In the transition metals, there is frequently no interaction between plane-wave and $3d$-type states at symmetry points in the Brillouin zone, so the bands of one type are virtually unaffected by the presence of the other. These bands do interact along lines of symmetry and at more general points in the Brillouin zone, but it is still profitable to think in terms of unperturbed plane-wave and $3d$ bands and discuss the s-d interaction, much in the way Slater and Koster[16] and more recently Lomer[17] have done.

In the case of the V_3X compounds having the β-wolfram structure, the vanadium $3d$ and plane-wave type states usually interact even at symmetry points in the Brillouin zone, so it is considerably more difficult to untangle the results and less meaningful to talk in terms of $3d$, plane-wave, or other types of bands. Nevertheless, a crude separation of this sort can be made for these compounds; this simplifies the general interpretation and discussion of the results to a considerable extent. In carrying out such a separation, it

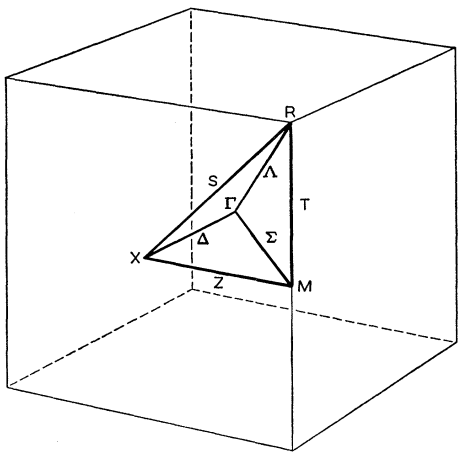

FIG. 2. The Brillouin zone for the simple-cubic Bravais lattice, using the notation of Bouckaert, Smoluchowski, and Wigner to label symmetry points and lines.

[16] J. C. Slater and G. F. Koster, Phys. Rev. **94**, 1498 (1954).
[17] W. M. Lomer, Proc. Phys. Soc. (London) **80**, 489 (1962).

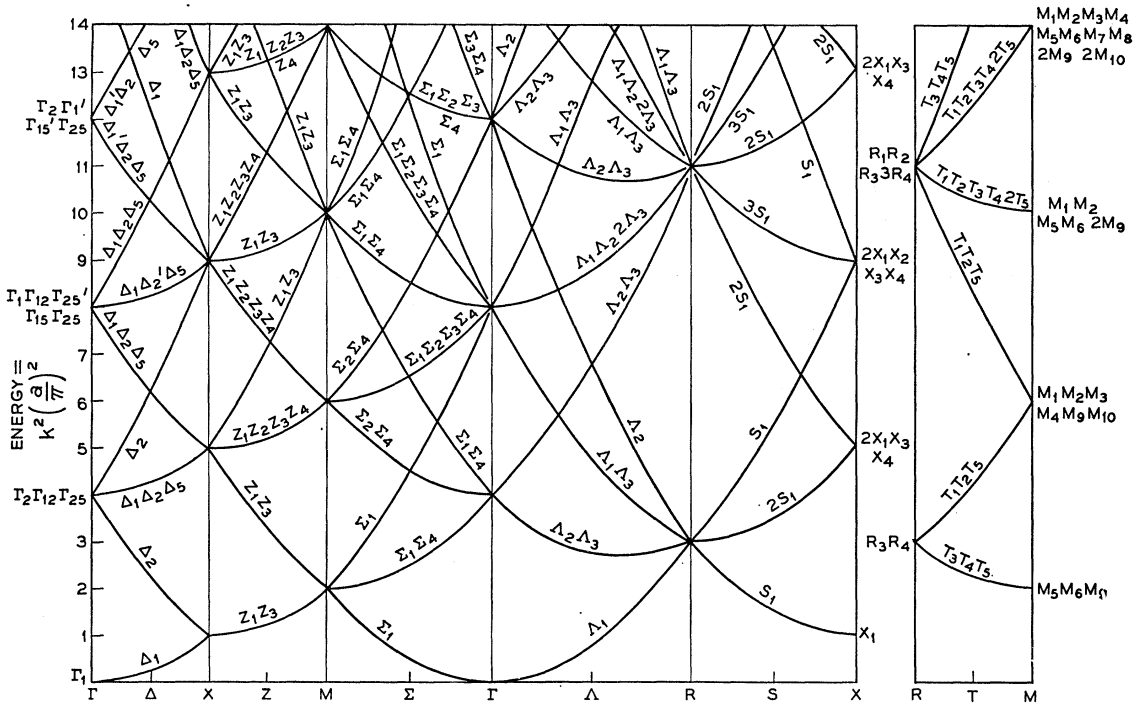

FIG. 3. The free-election energy bands for the β-wolfram structure along symmetry directions in the Brillouin zone. The energy is in units $n^2=(a/\pi)^2k^2$.

is necessary to know which spherical harmonics are contained in an APW wave function of a given symmetry. This information is summarized in Table IV for the irreducible representations at symmetry points in the Brillouin zone for the β-wolfram structure. This analysis is best understood in terms of the tight-binding approximation. It specifies which tight-binding functions (formed from the various atomic orbitals) are associated with a given irreducible representation of the space group O_h^3 for the β-wolfram structure.

Slater, in his original formulation of the APW method, treated a general crystal structure containing an arbitrary number of atoms per unit cell,[7] although the first applications of the method have been to the body- and face-centered cubic structures.[8,9] In applying the method, it is convenient (though not necessary) to approximate the actual crystal potential by a "muffin-tin" potential. This "muffin-tin" potential consists of spheres surrounding each atomic site in which the potential is assumed to be spherical and regions between the spheres where the potential is assumed to be constant. Different atoms can have different sphere radii, though it is advantageous to make the spheres as large as possible for a given structure. The value chosen for the constant potential between the APW spheres is generally the average value of the potential in this region.

The manner in which symmetry has been incorporated into the APW method for the body- and face-centered cubic structures has been described by Wood.[9] The extension of Wood's symmetrization techniques to

TABLE IV. The occurrence of low-order spherical harmonics in the APW wave functions for the β-wolfram structure at symmetry points in the Brillouin zone. Blank entries represent spherical harmonics which are absent by symmetry.

	B Atoms			*A* Atoms		
Point Γ	$l=0$	$l=1$	$l=2$	$l=0$	$l=1$	$l=2$
Γ_1	s			s		d
$\Gamma_{1'}$						d
Γ_2	s				p	d
$\Gamma_{2'}$						
Γ_{12}			$2d$	s	p	$2d$
$\Gamma_{12'}$						d
Γ_{25}		p		s	p	$2d$
$\Gamma_{25'}$			d		p	$2d$
Γ_{15}		p			$2p$	$2d$
$\Gamma_{15'}$			d		p	d
Point X						
X_1	s	p	$2d$	$2s$	$3p$	$5d$
X_2			d		p	$3d$
X_3		p	d	s	$2p$	$4d$
X_4		p	d		$3p$	$3d$
Point M						
M_1		p		s	p	$2d$
M_2		p			$2p$	$2d$
M_3			d		p	$2d$
M_4			d	s		$2d$
M_5		p		s	p	$3d$
M_6		p		s	p	$2d$
M_7			d		p	d
M_8			d		p	$2d$
M_9	s		$3d$	s	$3p$	$4d$
M_{10}		p			$2p$	$3d$
Point R						
R_1			d		p	d
R_2			d		p	d
R_3	s				p	d
R_4		p	d	s	$2p$	$4d$

a compound containing N atoms per unit cell is straightforward. Switendick has written general APW computer programs which can handle structures containing two different types of atoms per unit cell,[10] provided the structure has inversion symmetry. (The Hamiltonian matrix can be made real for structures with inversion symmetry.) Switendick's programs are readily adapted to any such compound by introducing the appropriate structure factor plus some other minor changes.

Aside from the ease with which the APW method can be adapted to a particular crystal structure, the method has another advantage which favors its application to compounds of the β-wolfram type. Namely, the method converges fairly rapidly, not only for broad plane-wave type bands, but also for narrow d bands. One possible drawback to the method, as it has been applied here, involves the "muffin-tin" potential approximation. The use of a "muffin-tin" potential for these V_3X compounds is clearly less satisfactory than in the case of the transition metals since the V atoms are situated at sites of rather low symmetry. The assumption of a spherically symmetric potential inside the APW spheres is probably quite reasonable for X atoms, though it is more questionable in the case of the V atoms. Furthermore, one can expect significant differences between the actual potential and the constant value that is assumed in the region between the APW spheres. Since the vanadium $3d$ wave functions have their maxima inside the APW spheres and only their "tails" extend into the region between spheres, the $3d$ bands are probably less affected by this approximation. Thus, one might expect that the principal errors introduced by the "muffin-tin" approximation affect the $3d$ bandwidth and the positioning of the $3d$ bands with respect to the plane-wave and other types of bands. This is not a serious limitation since these parameters are uncertain in all energy-band calculations which involve d electrons; in the case of the transition metals, the correct s-d energy separation is usually inferred from experiment.

For these V_3X compounds, one can construct touching APW spheres around the V atoms with radii $R_v = a/4$. This is shown in Fig. 1. The APW spheres around the X atoms will touch the V atom APW spheres when $R_x = \frac{1}{4}(\sqrt{5}-1)a$. In this case, approximately 64% of the total volume of the unit cell is contained within the six V atom and two X atom APW spheres. This compares favorably with the 74 and 68% which result from touching spheres in the face-centered and body-centered cubic structures, respectively.

The approximate crystal potentials used in the present calculations have been obtained in a manner analogous to that described earlier for calculations on transition metals.[18,19] The method involves the superposition of Coulomb potentials and charge densities of the appropriate Hartree-Fock atomic solutions situated at their appropriate sites in the lattice, spherically averaged to yield spherically symmetric functions inside a given APW sphere. Exchange has been introduced by means of the Slater free-electron exchange approximation,[20] being proportional to the cube root of the superimposed charge densities. Thus, the vanadium potentials for the various V_3X compounds differ slightly, these differences being due to small changes in the lattice constants and differences in the tails of the X atoms which extend into the vanadium APW spheres.

Unpublished calculations on several transition metals by the author indicate that equivalent energy bands are obtained if one uses the Hartree-Fock-Slater atomic solutions as obtained by Herman and Skillman[21] instead of the Hartree-Fock solutions, and these have been used in the present series of calculations. Also, the APW sphere radii for the X atoms have not been taken as the maximum value $R_x = \frac{1}{4}(\sqrt{5}-1)a$ in these calculations. Rather, these radii have been determined by the condition that the potential at the X atom sphere radius equal that at the vanadium sphere radius, $R_v = \frac{1}{4}a$. Table V contains the values of R_x used in the calculations for the various V_3X compounds, as well as other pertinent information such as the assumed atomic configuration, the number of electrons per unit cell, and the lattice constant a. These lattice constants, with the exception of that for hypothetical V_3Al, were the room-temperature values tabulated by Pearson.[22] These were found to differ in some cases from the values quoted by Matthias, Geballe, and Compton.[1] However, since the results appear to be insensitive to small changes in the lattice constant, these differences are not very significant. The lattice constant for hypothetical V_3Al has been estimated by comparing the lattice constants for V_3Si, V_3Ga, and V_3Ge and carrying out a reasonable extrapolation.

TABLE V. The assumed atomic configurations, the number of electrons per unit cell, the lattice constants a (in atomic units), and the X atom sphere radii (also in atomic units) which have been used in the present series of APW energy-band calculations for the V_3X compounds, where the X atoms include Al, Si, Co, Ga, Ge, and As.

V_3X	Configuration V	Configuration X	No. of electrons per unit cell	Lattice constant a (atomic units)	R_x (atomic units)
V_3Al	$(3d)^4(4s)^1$	$(3s)^2(3p)^1$	36	9.038	2.383
V_3Si	$(3d)^4(4s)^1$	$(3s)^2(3p)^2$	38	8.923	2.463
V_3Co	$(3d)^4(4s)^1$	$(3d)^8(4s)^1$	48	8.835	2.049
V_3Ga	$(3d)^3(4s)^2$	$(4s)^2(4p)^1$	36	9.127	2.380
V_3Ga	$(3d)^4(4s)^1$	$(4s)^2(4p)^1$	36	9.127	2.166
V_3Ge	$(3d)^4(4s)^1$	$(4s)^2(4p)^2$	38	9.012	2.482
V_3As	$(3d)^4(4s)^1$	$(4s)^2(4p)^3$	40	8.976	2.499

[18] L. F. Mattheiss, Phys. Rev. **133**, A1399 (1964).
[19] L. F. Mattheiss, Phys. Rev. **134**, A970 (1964).
[20] J. C. Slater, Phys. Rev. **81**, 385 (1951).
[21] F. Herman and S. Skillman, *Atomic Structure Calculations* (Prentice-Hall, Inc., Englewood Cliffs, New Jersey, 1963).
[22] W. B. Pearson, *A Handbook of Lattice Spacings and Structures of Metals and Alloys* (Pergamon Press, Inc., New York, 1958).

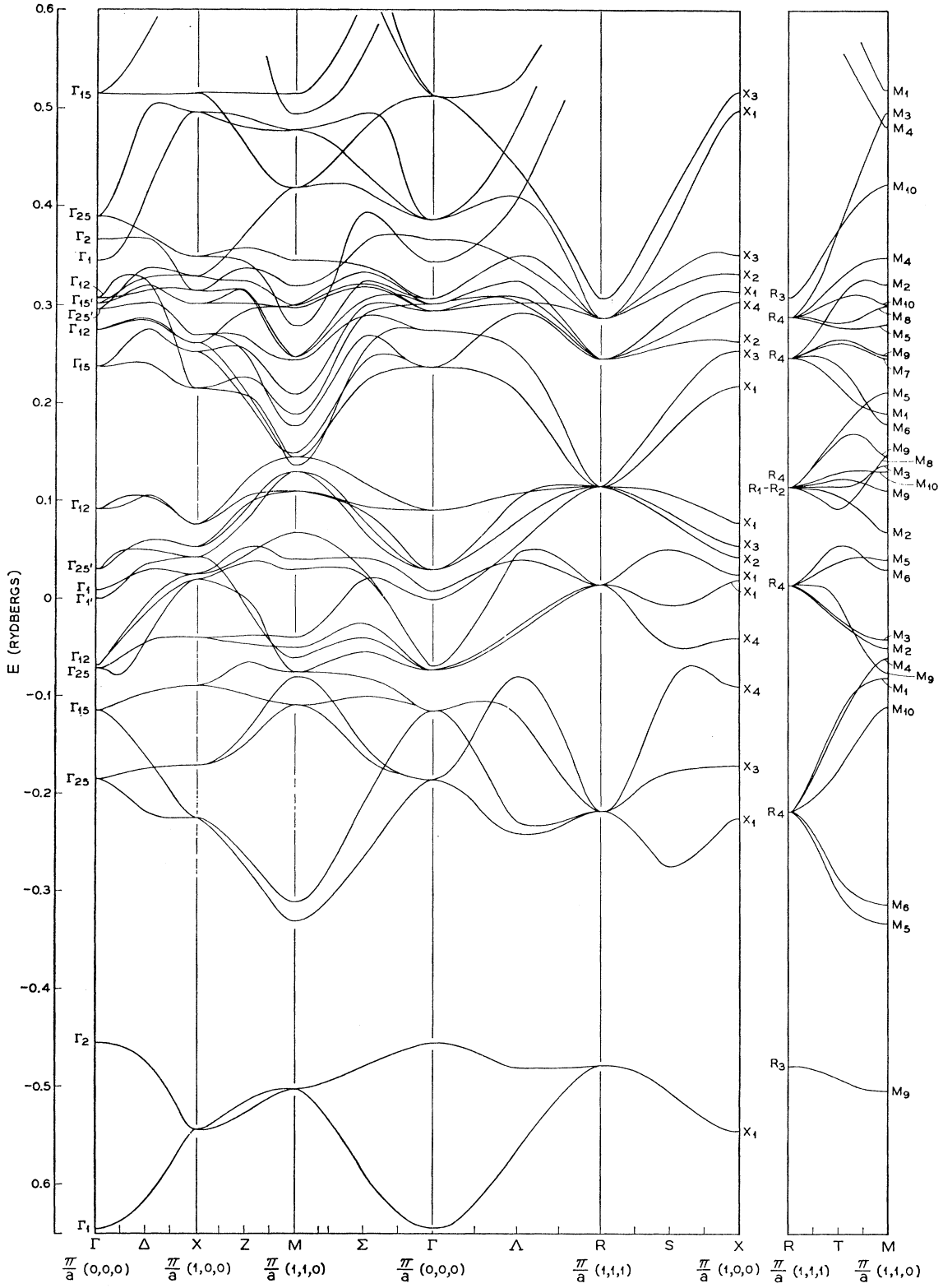

FIG. 4. $E(k)$ curves for V_3Ga along symmetry directions in the Brillouin zone. The energy is in Rydbergs.

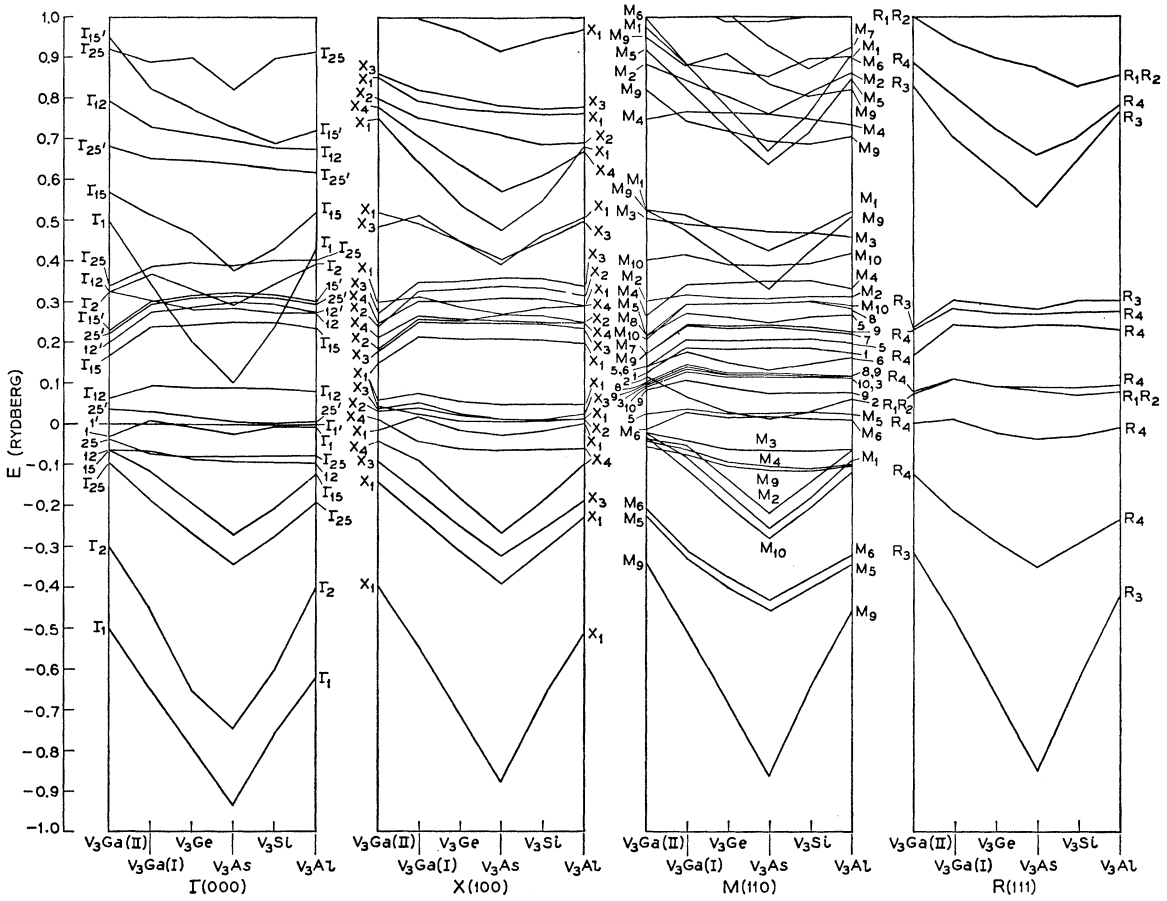

FIG. 5. Energy eigenvalues at the symmetry points Γ, X, M, and R plotted as a function of the X atoms, including results for V_3Ga (two potentials), V_3Ge, V_3As, V_3Si, and V_3Al.

III. APW RESULTS

The energy bands $E(\mathbf{k})$ for V_3Ga are plotted along symmetry directions in the simple cubic Brillouin zone in Fig. 4. The energy is in Rydbergs, and the zero of energy has been chosen to coincide with the energy eigenvalue for the state with $\Gamma_{1'}$ symmetry, $E(\Gamma_{1'})$. Since the APW calculations have been carried out only at symmetry points and at the midpoints of the symmetry lines for V_3Ga, the smooth curves in Fig. 4 represent a free-hand interpolation between this limited set of points such that the compatibility relations are satisfied. Convergence studies indicate that the APW energy eigenvalues are converged to within 0.01 Ry at symmetry points in the Brillouin zone. For reasons of economy, this accuracy was sometimes reduced to 0.02 Ry along symmetry lines and this has undoubtedly introduced some structure into the $E(\mathbf{k})$ curves shown in Fig. 4. Along the symmetry line S, it proved to be very impractical to calculate results which were converged to 0.02 Ry; as a consequence, the curves along the S direction in Fig. 4 are merely sketched in, using the unconverged results as a guide.

In the energy range of 1.2 Ry which is spanned in Fig. 4, there are approximately forty bands. These have been identified only at symmetry points, for obvious reasons. The identification of bands along symmetry lines can usually be accomplished by means of the compatibility relations of Table III, though some ambiguities exist. Since we shall concern ourselves only with the gross features of these results, these ambiguities are not important in the following discussions.

Before attempting to comment on these results in any detail, it is useful to compare these calculations for V_3Ga with the analogous results for the other V_3X compounds. This is done in Fig. 5. Here, the energy-band results at the symmetry points Γ, X, M, and R are plotted as a function of the X atom for a number of V_3X compounds. At each symmetry point, the left-hand results represent the energy-band states for V_3Ga. These have been calculated using two different vanadium potentials. These potentials have been obtained by assuming different atomic configurations for vanadium, namely $(3d)^3(4s)^2$ and $(3d)^4(4s)^1$. The notation V_3Ga-(II) and V_3Ga(I) is used to distinguish between these two calculations, the Roman numeral in parentheses

indicating the number of vanadium $4s$ electrons. The energy bands shown in Fig. 4 correspond to V_3Ga(I). In Fig. 5, the results to the right of those for V_3Ga are those for V_3Ge, V_3As, V_3Si, and hypothetical V_3Al, respectively. These latter results have all been obtained using a vanadium potential which corresponds to a $(3d)^4(4s)^1$ atomic configuration and the appropriate configuration for the corresponding X atom.

The combined results of Figs. 4 and 5 permit one to understand some of the gross features of these rather complicated energy bands. The lowest pair of bands (Γ_1,Γ_2; X_1; M_9; R_3) are presumably associated with the X atom s electrons, the next six bands (Γ_{25},Γ_{15}; X_1,X_3,X_4; M_5,M_6,M_{10},M_1,M_2; R_4) with the X atom p electrons. The next group of bands which are connected by the approximately parallel lines in Fig. 5 correspond to the vanadium $3d$ bands. This interpretation is consistent with the results of the group-theoretical analysis which are summarized in Table IV. In plotting Figs. 4 and 5, the zero of energy has been taken at $E(\Gamma_{1'})$ since there is a single vanadium $3d$-band state with this symmetry and there are no other states of the same symmetry in the immediate energy range. It therefore represents a convenient reference energy for comparing these different V_3X calculations.

An interesting feature of the vanadium $3d$ bands is the fact that they appear to be divided into two sub-bands, separated by a minimum in the density of states. This division occurs in the energy range from 0.1 to 0.2 Ry in Figs. 4 and 5. It occurs at the symmetry points Γ, X, and R in the Brillouin zone, though not at M. From Fig. 4 it is seen that there are no states crossing from one sub-band to the other along the Δ direction in the Brillouin zone. Energy-band states do pass through this energy range along other symmetry and nonsymmetry directions in the Brillouin zone. However, since these bands have appreciable slope in this region, their contribution to the density of states is expected to be small.

This division of the vanadium $3d$ bands into two sub-bands is an important feature of the β-wolfram structure since the Fermi energy for V_3Ga falls near the top of the lower sub-band. In view of this striking result, an attempt has been made to isolate those interactions responsible for this $3d$-band structure. One aspect of this investigation involves a series of calculations for V_3Ga in which either the vanadium or gallium atoms have been omitted from the β-wolfram structure. With the vanadium atoms omitted, the gallium atoms form a body-centered cubic lattice. The eigenvalues for body-centered cubic gallium have been obtained using the β-wolfram APW program, modified to omit the vanadium atoms. The gallium potential and lattice constant were identical to those used in the V_3Ga(I) calculation. When these same potentials and lattice constants were assumed in a similar calculation using Wood's body-centered APW program,[9] identical results were obtained. This agreement constitutes an excellent test of the β-wolfram APW program and an over-all check on the group-theoretical analysis for the space group O_h^3. The energy bands for body-centered gallium are found to be rather free-electron like, the energy gaps introduced by the Fourier coefficients of the potential being of the order of 0.1 Ry.

The more interesting results are those obtained from calculations on hypothetical V_3 in which the gallium atoms are omitted from the β-wolfram structure. In a series of such calculations on V_3, the constant potential between the APW spheres V_c has been varied from -1.39 Ry (the value appropriate for V_3Ga) to -0.89 Ry and finally to -0.39 Ry. The results of these calculations are presented in Fig. 6, where again the zero of energy has been taken at $E(\Gamma_{1'})$. In this figure, the energy bands for V_3Ga are compared with those for V_3 at the various symmetry points in the Brillouin zone as a function of V_c, the constant value of the "muffin-tin" potential between the APW spheres. The first interesting point to be noticed from this figure is the fact that the $3d$ bands are not greatly affected by the absence of the gallium atoms. This result precludes the possibility that the $3d$ structure is due to interactions between the vanadium $3d$ and gallium $4s$ or $4p$ bands. This result may also be inferred from Fig. 5, where the $3d$-band structure is relatively insensitive to considerable variations in the s-d or p-d energy separations. Secondly, the $3d$ bands narrow as the constant potential between the APW spheres is raised. This is an expected result since raising the potential outside the vanadium spheres places the $3d$ electrons in a deeper and deeper potential well, and this causes them to become more localized. Third, since the $3d$-band structure is rather insensitive to the vanadium s-d energy separation, it is probably not due to vanadium s-d interactions. Finally, the energy separation between the two vanadium $3d$ sub-bands is approximately proportional to the total $3d$ bandwidth. This result suggests that the division of the vanadium $3d$ bands into two sub-bands is due to vanadium d-d interactions. Since we shall show in the following section that nearest-neighbor interactions cannot account for this division, we must conclude that it is due to second- or higher-neighbor interactions.

It is interesting to contrast the energy bands shown in Figs. 4 and 5 with those obtained for V_3Co. The latter results are presented in Fig. 7. Since these calculations have been carried out only at symmetry points in the Brillouin zone, the bands along symmetry lines are merely sketched in such that they are consistent with the compatibility relations. The high density of energy-band states prevents any serious errors in such a free-hand interpolation process. These energy bands for V_3Co differ from those shown in Figs. 4 and 5 in three respects. First, the thirty vanadium $3d$ bands are now overlapped by the ten cobalt $3d$

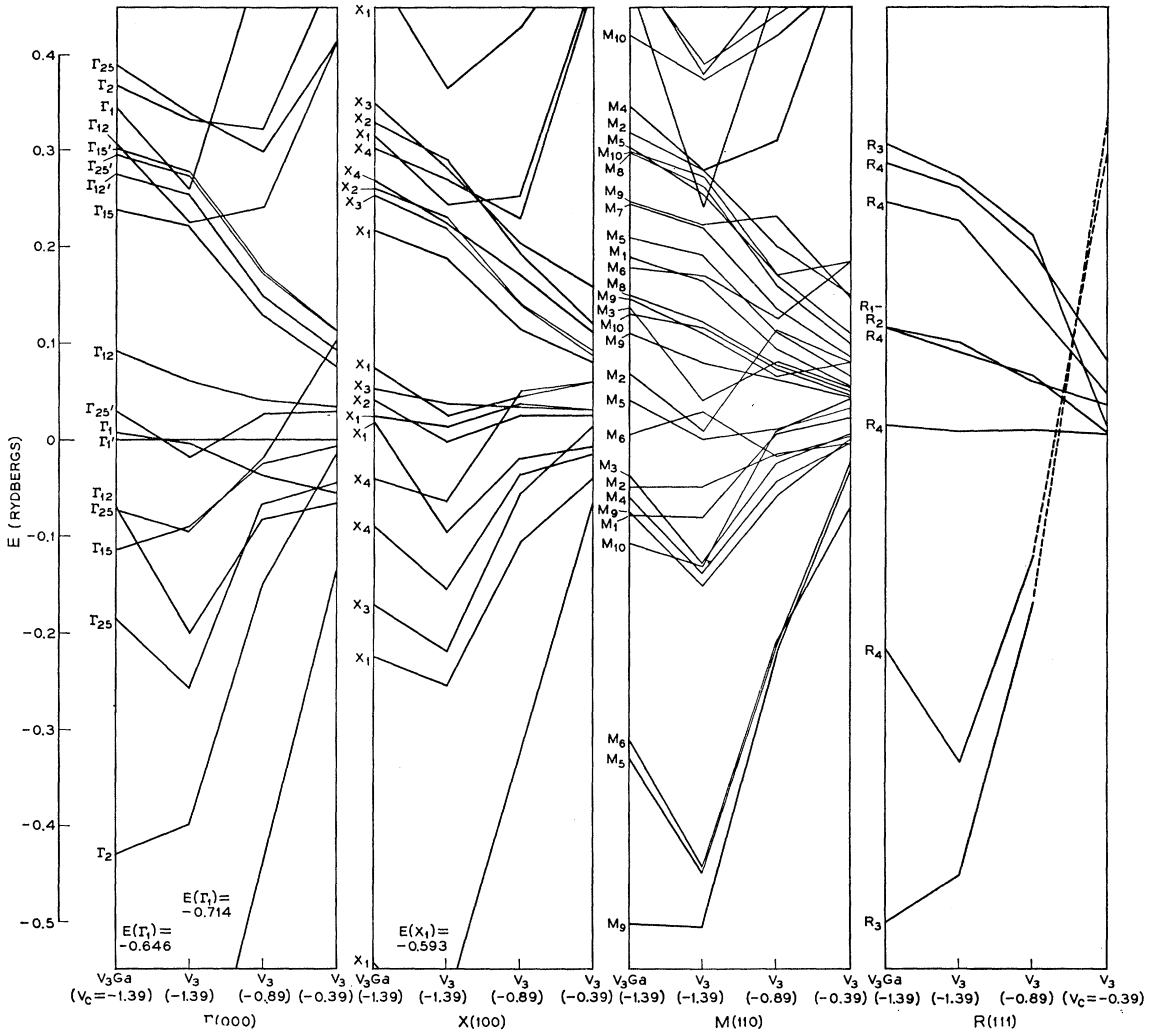

FIG. 6. Comparison between the energy-band states for V_3Ga and hypothetical V_3 at symmetry points in the Brillouin zone as a function of the constant potential between the APW spheres.

bands. By comparing Figs. 4, 5, and 7 it is clear that the cobalt 3*d* bands lie near the bottom of the vanadium 3*d* bands, as they should. Second, it appears that the interaction between vanadium and cobalt 3*d* bands is stronger than that between vanadium 3*d* and *X* atom *s* and *p* bands. Third, the bands above and below the combined cobalt and vanadium 3*d* bands are more free-electron like in character than those shown in Figs. 4 and 5. This is evident from a comparison between Fig. 7 and free-electron bands shown in Fig. 3.

Of course, the separation of the energy-band results of Figs. 4 and 5 into *X* atom *s* and *p* bands and vanadium 3*d* bands should not be taken too literally, since there will clearly be mixing between the various bands. The extent to which this mixing occurs in any given band can be determined by examining the corresponding APW wave functions. These APW wave functions are composite in nature, being expanded in terms of spherical harmonics inside the APW spheres and plane waves in the region between spheres. When the APW function is normalized over a unit cell, the normalization integral yields the fractional charge associated with each spherical harmonic inside the six V atom and two *X* atom spheres as well as the fractional charge between the spheres.

Some typical results that have been obtained from a wave function analysis for V_3Ga(I) and V_3Ga(II) are included in Tables VI and VII. Table VI contains some limited results for V_3Ga(I), including states which transform like Γ_1, Γ_2, and $\Gamma_{1'}$. In Table VII the wave functions with X_1 symmetry for V_3Ga(I) are compared with those for V_3Ga(II). The entries under PW represent the fractional charge contained in the plane-wave region between the APW spheres. Similarly, the entries under Ga and V represent the fractional *s*, *p*, or *d* charge that is contained within the two gallium or six

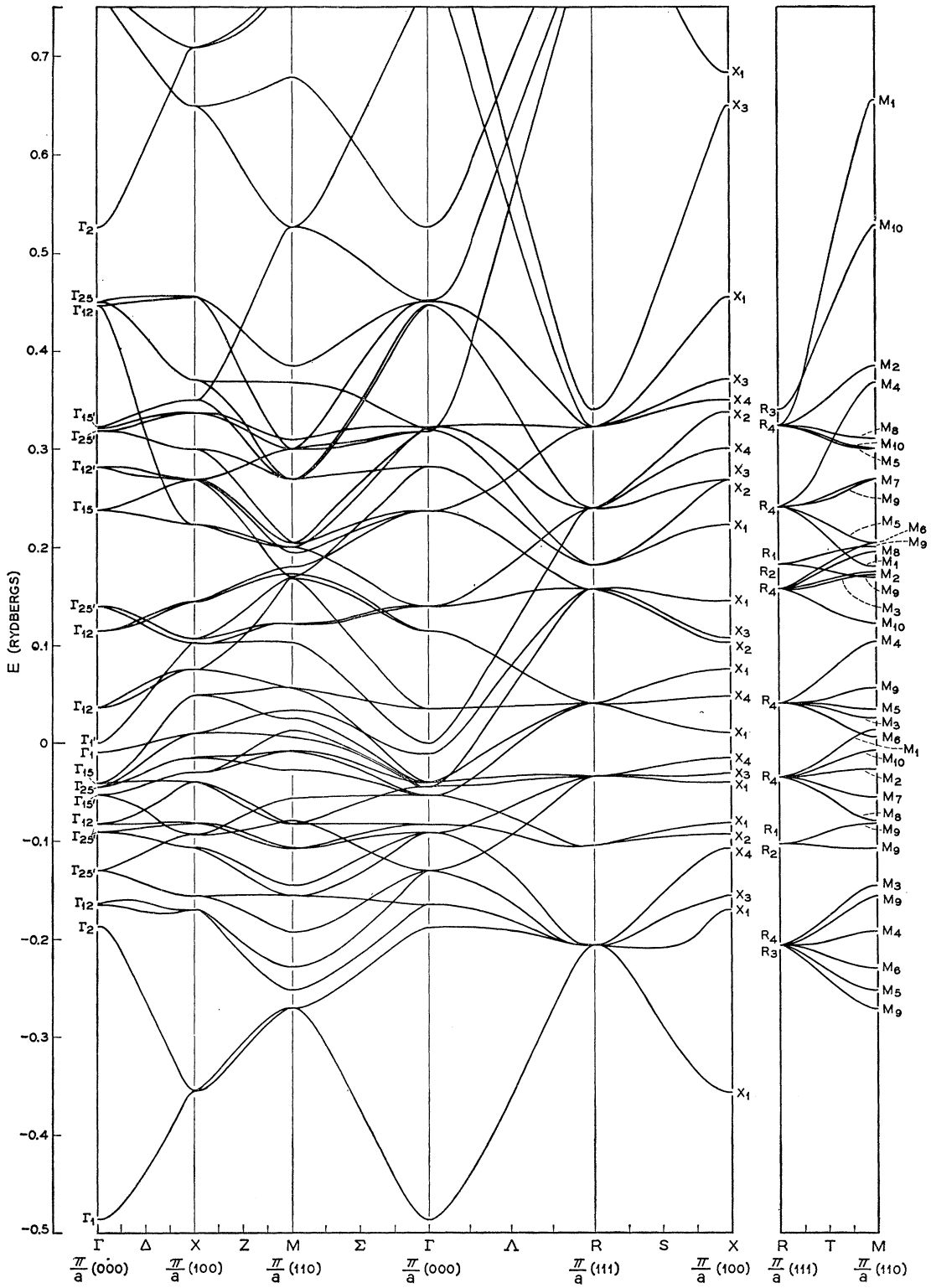

FIG. 7. $E(k)$ along symmetry directions for V_3Co. The energy is in Rydbergs, and the $E(k)$ curves are merely sketched in so that they are consistent with the compatibility relations.

TABLE VI. Analysis of V_3Ga(I) APW wave functions for states with Γ_1, Γ_2, and $\Gamma_{1'}$ symmetry. The entries under PW represent the fractional charge in the plane-wave region between the APW spheres. The entries under Ga and V represent the fractional charge inside the two gallium and six vanadium APW spheres that is associated with a given spherical harmonic in the APW expansion.

			Ga			V		
State	Energy	PW	4s	4p	4d	4s	4p	3d
Γ_1	−0.646	0.488	0.320	···	···	0.187	···	0.004
Γ_2	−0.456	0.342	0.493	···	···	···	0.035	0.128
$\Gamma_{1'}$	0.000	0.279	···	···	···	···	···	0.712
Γ_1	0.008	0.152	0.014	···	···	0.049	···	0.780
Γ_1	0.344	0.345	0.362	···	···	0.171	···	0.089
Γ_2	0.367	0.029	0.114	···	···	···	0.004	0.852
Γ_2	1.067	0.358	0.046	···	···	···	0.546	0.009

vanadium spheres. A total of 13 spherical harmonics have been included in the present series of calculations. Those fractions which do not add up to 1.0 contain some admixture of these higher spherical harmonics, which in general proves to be small. Blank entries represent spherical harmonics which are absent because of symmetry (see Table IV).

While the results contained in Tables VI and VII represent only two points in the Brillouin zone, limited sampling at other points suggests that these results are fairly representative examples of the wave-function character in any given energy range. These results indicate that there is considerable admixture in the bands which previously have been identified as gallium 4s and 4p and vanadium 3d bands on the basis of group-theoretical arguments. The lowest pair of bands (Γ_1,Γ_2; X_1), which previously have been associated with the gallium 4s electrons, are found to contain significant fractions of vanadium 4s, 4p, and even 3d charge. The same situation exists for the next group of bands that have been associated with the gallium 4p electrons. The second state with X_1 symmetry in Table VII contains only 15% gallium 4p character in the case of V_3Ga(I) and 5% in the case of V_3Ga(II). To a certain extent, the differences between the results for V_3Ga(I) and V_3Ga(II) are due to the fact that the gallium sphere radius is about 10% smaller in the latter case.

As one moves into the energy range of the vanadium 3d bands, the fractional vanadium 3d charge increases noticeably, especially near the center of the band. There is a corresponding decrease in the fractional charge outside the spheres. This reflects the fact that the vanadium 3d functions are more localized than the 4s- and 4p-type functions. The radial 3d functions have their maxima inside the vanadium APW spheres, and only their "tails" extend into the regions between spheres. The outermost maxima for the vanadium and gallium 4s- and 4p-type functions occur in the plane-wave region, and this accounts for the increased charge in this region when the admixture of these functions is increased.

These limited results concerning the APW wave functions for V_3Ga provide additional insight into the nature of the energy bands for these V_3X compounds. For instance, they suggest a reasonable explanation for the behavior of the state with Γ_1 symmetry which cuts through the energy range of the vanadium 3d bands in V_3Ga, V_3Ge, and V_3As, as shown in Fig. 5. According to the results of Table VI, this state contains approximately the same admixture of gallium and vanadium 4s-type charge as the lowest Γ_1 state. As the X atom 4s band becomes more tightly bound, this upper Γ_1 state presumably drops below the vanadium 3d bands and becomes the bottom of the vanadium 4s conduction band. Comparison of the results for V_3Ga(I)

TABLE VII. Analysis of the V_3Ga(I) and V_3Ga(II) APW wave functions for states with X_1 symmetry.

			Ga			V		
	Energy	PW	4s	4p	4d	4s	4p	3d
V_3Ga(I)	−0.546	0.448	0.371	0.009	0.000	0.107	0.039	0.026
	−0.225	0.438	0.063	0.128	0.003	0.113	0.012	0.240
	0.019	0.337	0.013	0.037	0.009	0.045	0.072	0.480
	0.024	0.234	0.003	0.001	0.000	0.019	0.037	0.700
	0.076	0.248	0.001	0.013	0.020	0.015	0.055	0.644
	0.217	0.105	0.000	0.008	0.008	0.006	0.028	0.836
	0.316	0.170	0.033	0.004	0.030	0.041	0.045	0.670
	0.497	0.231	0.109	0.005	0.029	0.114	0.069	0.433
	0.65	0.282	0.066	0.184	0.004	0.087	0.071	0.279
	0.799	0.366	0.006	0.016	0.053	0.142	0.101	0.279
	0.999	0.395	0.000	0.082	0.070	0.072	0.271	0.056
V_3Ga(II)	−0.392	0.532	0.254	0.007	0.000	0.130	0.040	0.035
	−0.144	0.398	0.037	0.054	0.002	0.097	0.006	0.405
	−0.016	0.128	0.000	0.005	0.001	0.011	0.002	0.851
	0.041	0.265	0.017	0.027	0.003	0.009	0.048	0.625
	0.059	0.239	0.006	0.000	0.005	0.019	0.059	0.667
	0.151	0.083	0.000	0.005	0.002	0.005	0.020	0.878
	0.302	0.266	0.065	0.020	0.017	0.053	0.099	0.474
	0.523	0.215	0.062	0.013	0.015	0.107	0.052	0.532
	0.755	0.367	0.112	0.155	0.005	0.086	0.103	0.146
	0.856	0.450	0.032	0.005	0.033	0.165	0.124	0.155
	1.096	0.437	0.000	0.108	0.044	0.060	0.258	0.040

and hypothetical V_3 in Fig. 7 supports this interpretation. In general, the wave-function analysis of Tables VI and VII suggests that there is considerable admixture in the bands which previously have been identified as X atom s and p and vanadium $3d$ bands on the basis of group-theoretical arguments. The charge distributions for either V_3Ga(I) or V_3Ga(II) are roughly consistent with our initial assumption of neutral vanadium and gallium atoms in the calculation of the potential. Finally, these APW calculations for V_3Ga(I) and V_3Ga(II) predict that the admixture of gallium $4p$ wave function in the vicinity of the Fermi energy is small. This result is at variance with the energy-band model for V_3Ga that has been proposed by Clogston and Jaccarino to explain the negative Knight shift at the gallium site. The amount of gallium $4p$ character at the Fermi energy is not enhanced appreciably by small adjustments to the vanadium and gallium potentials or changes in the APW sphere radius at the gallium site.

A rather crude density-of-states calculation has been carried out for V_3Ga(I), using the results of Fig. 4. Graphical interpolation has been used to obtain approximate eigenvalues at more general points in the interior of the Brillouin zone. In view of the large number of bands involved and the uncertainties inherent in such an interpolation procedure, this density-of-states calculation has been limited so as to include only 514 points in the Brillouin zone. This is equivalent to subdividing the Brillouin zone into cubes whose edge dimensions are $\frac{1}{4}(\pi/a)$. Such a density-of-states calculation is expected to be crude, though it should reflect some of the gross features of these energy-band calculations for V_3Ga(I).

The density-of-states curve for V_3Ga(I) which results from this calculation is shown in Fig. 8. This curve is in the form of a histogram, using an energy mesh $\Delta E=0.02$ Ry. This figure includes a total of 36 bands and extends over an energy range which includes most of the gallium $4s$ and $4p$ bands as well as the vanadium $4s$, $4p$, and $3d$ bands. The dashed line in Fig. 8 indicates the number of electrons per unit cell that are available at a given energy. From this figure, the Fermi energy for V_3Ga(I) is estimated to be 0.10 Ry. Assuming a rigid-band model, the Fermi energies for V_3Ge and V_3As are estimated to be 0.11 and 0.14 Ry, respectively. The Fermi energies for V_3Ga and V_3Ge coincide with the peak in the density-of-states curve which occurs just before the minimum at 0.15 Ry. The Fermi energy for V_3As falls near the minimum itself.

Weger[12] has proposed a simple Fermi-surface model for V_3Ga and V_3Si. From his tight-binding analysis, he finds a $3d$ Fermi surface which, in an extended zone scheme, corresponds to closed, cube-shaped hole surfaces about the point R in the Brillouin zone. Although the accuracy of the present APW calculations is sufficiently uncertain to discourage any detailed description

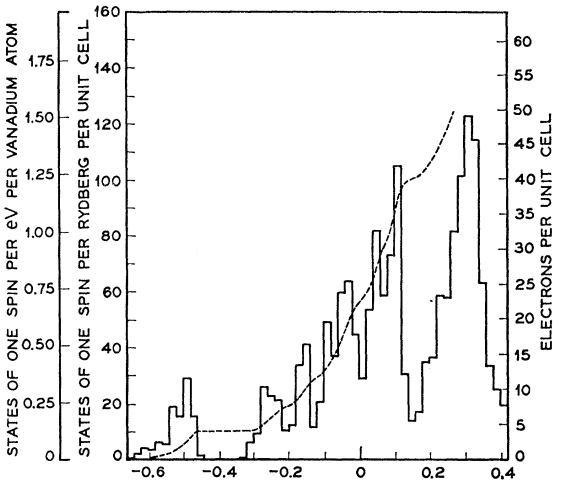

FIG. 8. Density-of-states curve for V_3Ga, using an energy mesh of 0.02 Ry. To the left, the units are spin states per eV per vanadium atom and spin states per Rydberg per unit cell, respectively. The dashed line is the integrated curve, the scale to the right indicating the number of electrons that can be accommodated at a given energy.

of the corresponding Fermi surfaces, it is perhaps worthwhile pointing out that a total of six Fermi surfaces are predicted. The first surface consists of hole pockets around R. The second contains hole pockets at the points R and M, which may or may not be connected along the line T. The third and fourth Fermi surfaces contain similar hole pockets at R and M which are connected along T, resulting in hole tubes along the edges of the Brillouin zone. The fifth and sixth Fermi surfaces consist of electron pockets around Γ which may or may not be connected to similar pockets at X, the center of the Brillouin zone face. If the Fermi energy has been chosen correctly, the volume of the electron pockets for the last two Fermi surfaces will equal the combined volumes of the hole pockets for the first four Fermi surfaces. An interesting feature of these Fermi surfaces is the fact that open orbits are possible along the $\langle 100\rangle$ axes for the third and fourth Fermi surfaces and perhaps some of the others. Weger's model does not predict open orbits.

The APW results described in this section have been obtained using approximately 200 unsymmetrized APW basis functions. This corresponds roughly to all those plane waves whose square magnitude $n^2=k^2(a/\pi)^2\leq 50$. Convergence studies indicate that this number of basis functions is sufficient to insure convergence to approximately 0.01 Ry. Table VIII contains the results of some convergence studies which have been carried out at the point Γ for V_3Ga(I). These results indicate that some eigenvalues converge faster than others. This can be understood in terms of the relatively poor convergence of states associated with the $3d$ bands as compared to s- or p-band states. For calculations along symmetry directions, the increased size of the secular equation made it desirable to sacrifice some accuracy in the

TABLE VIII. Convergence of APW energy eigenvalues at the point Γ in the Brillouin zone for V_3Ga(I). The quantity n^2 is $(a/\pi)^2k^2$; the corresponding entries under No. represent the total number of unsymmetrized APW basis functions which are associated with a given value of n^2.

n^2	100	90	80	70	60	40	20
No.	515	461	389	305	251	147	57
Γ_1	−0.6462	−0.6462	−0.6462	−0.6462	−0.6462	−0.6461	−0.6459
	0.0010	0.0016	0.0019	0.0042	0.0082	0.0115	0.0806
	0.3421	0.3422	0.3422	0.3426	0.3435	0.3436	0.3506
Γ_2			−0.4561		−0.4556	−0.4547	−0.4502
			0.3618		0.3672	0.3739	0.4487
Γ_{12}			−0.0715		−0.0686	−0.0665	−0.0222
			0.0861		0.0921	0.0990	0.1281
			0.3020		0.3066	0.3128	0.3589
			0.7286		0.7300	0.7319	0.7737

interest of program efficiency and economy. An extreme situation arises along the S direction in the Brillouin zone, where it is necessary to solve a 75×75 secular equation in order to obtain results which are converged to approximately 0.01 Ry. Although such a secular equation is not beyond the capabilities of Switendick's APW program, it would have required an estimated three hours of IBM 7094 time to carry it through. By comparison, the calculation of all the energy-band states at the four symmetry points Γ, X, M, and R for a given V_3X compound required approximately one hour of IBM 7094 time.

IV. THE LINEAR CHAIN MODEL

A distinctive feature of the β-wolfram structure V_3X is the existence of V atom chains along axes parallel to the edges of the cubic unit cell. The nearest neighbor distance between V atoms along these chains is about 10% smaller than the second-neighbor distance between V and X atoms and about 20% smaller than the third neighbor distance between V atoms belonging to different chains. This aspect of the β-wolfram structure has led to the suggestion that the electronic properties of these V_3X compounds can be interpreted in terms of a one-dimensional or linear chain model. Weger[12] has described the results of a tight-binding calculation for the vanadium $3d$ bands in which only nearest-neighbor interactions have been included. It is interesting to study the results predicted by this model and compare them with the APW results described in the previous section.

Slater and Koster[16] have analyzed the tight-binding method and have shown how it may be applied as an interpolation scheme. In the two-center approximation, the nearest-neighbor d interactions can be represented in terms of three parameters, $(dd\sigma)$, $(dd\pi)$, and $(dd\delta)$. The parameters $(dd\sigma)$ and $(dd\delta)$ are expected to be negative while $(dd\pi)$ is positive. The relative magnitudes of these parameters are such that for our purposes we can assume $|(dd\sigma)|=2|(dd\pi)|=5|(dd\delta)|$.

Associated with each of the six V atoms in the unit cell, there are five d functions whose angular dependence can be described by the polynomials $(3z^2-r^2)$, (x^2-y^2), xy, yz, and zx. A total of thirty Bloch-type tight-binding functions can be formed from these orbitals so that the corresponding secular equation which includes their interactions is a 30×30 equation. However, in the two-center, nearest-neighbor approximation, this 30×30 secular equation factors into fifteen 2×2 equations, of which only three are distinct. These are given by Eq. (1a), (1b), and (1c), respectively.

$$\det\begin{vmatrix} d_0-E & 2(dd\sigma)\cos\mathbf{k}\cdot\mathbf{R} \\ 2(dd\sigma)\cos\mathbf{k}\cdot\mathbf{R} & d_0-E \end{vmatrix}=0, \quad (1a)$$

$$\det\begin{vmatrix} d_0-E & 2(dd\pi)\cos\mathbf{k}\cdot\mathbf{R} \\ 2(dd\pi)\cos\mathbf{k}\cdot\mathbf{R} & d_0-E \end{vmatrix}=0, \quad (1b)$$

$$\det\begin{vmatrix} d_0-E & 2(dd\delta)\cos\mathbf{k}\cdot\mathbf{R} \\ 2(dd\delta)\cos\mathbf{k}\cdot\mathbf{R} & d_0-E \end{vmatrix}=0. \quad (1c)$$

There are a total of three equations of type (1a), six of type (1b), and six of type (1c). In these equations, d_0 represents the diagonal, one-center matrix element that is common to all thirty d functions and R is a vector from one V atom to its neighbor. The secular equations of Eq. (1) can be solved to yield the following eigenvalues:

$$E_\pm{}^\sigma=d_0\pm|2(dd\sigma)\cos\mathbf{k}\cdot\mathbf{R}|, \quad (2a)$$

$$E_\pm{}^\pi=d_0\pm|2(dd\pi)\cos\mathbf{k}\cdot\mathbf{R}|, \quad (2b)$$

$$E_\pm{}^\delta=d_0\pm|2(dd\delta)\cos\mathbf{k}\cdot\mathbf{R}|. \quad (2c)$$

The corresponding eigenfunctions are the sums and differences of the original basis functions.

By examining the eigenfunctions which correspond to a given eigenvalue in Eq. (2), it is possible to determine those linear combinations of degenerate functions which transform irreducibly under the operations in the space group $O_h{}^3$. In this manner, it is possible to determine which irreducible representations are to be associated with a given eigenvalue. The results of such an analysis at the point Γ in the Brillouin zone are summarized in Table IX. According to this table, the linear chain model for the β-wolfram structure predicts that at Γ, the lowest d-band states have an energy $E_-{}^\sigma$ and transform like Γ_1 and Γ_{12}, the next group of states transform like Γ_{25} and Γ_{15}, and so on.

TABLE IX. Correspondence between the d-band eigenvalues predicted by the linear-chain model for the β-wolfram structure and the transformation properties of the corresponding eigenfunctions at the point Γ in the Brillouin zone.

Energy	Symmetry	Degeneracy
E_+^σ	Γ_{25}	3
E_+^π	$\Gamma_{15'}$, $\Gamma_{25'}$	6
E_+^σ	$\Gamma_{1'}$, $\Gamma_{12'}$, Γ_{15}	6
E_-^σ	Γ_2, Γ_{12}, $\Gamma_{25'}$	6
E_-^π	Γ_{25}, Γ_{15}	6
E_-^σ	Γ_1, Γ_{12}	3

The energy bands predicted by this simplified tight-binding analysis are illustrated in Fig. 9, where the energy is plotted as a function of wave vector along the Δ, Σ, and Λ directions in the Brillouin zone. The degeneracy of the individual energy-band states is indicated by the numbers in parentheses. Comparison of these results with the distribution of levels in Figs. 4 and 5 suggests that this two-center, linear chain approximation provides an oversimplified representation of the vanadium $3d$ bands in these V_3X compounds.

The symmetrical nature of the bands shown in Fig. 9 is a result of the two-center approximation for off-diagonal and one-center approximation for diagonal matrix elements of the Hamiltonian operator in Eq. (1). The low point-group symmetry at a V atom site permits the fivefold degeneracy of the d levels to be removed by crystalline field effects. In the cubic transition metals, this splitting is typically a few hundredths of a Rydberg. In these V_3X compounds, this splitting may be two or three times as large, due to the small nearest-neighbor distance and the low symmetry at a V atom site. The number of disposable parameters in the tight-binding analysis can be increased substantially if the energy integrals $E_{n,m}(p,q,r)$ (as defined by Slater and Koster[16]) are considered and the two-center approximation is not introduced. However, even with these additional parameters, the nearest-neighbor approximation does not appear to yield an adequate representation of the vanadium $3d$ bands, as calculated by the APW method.

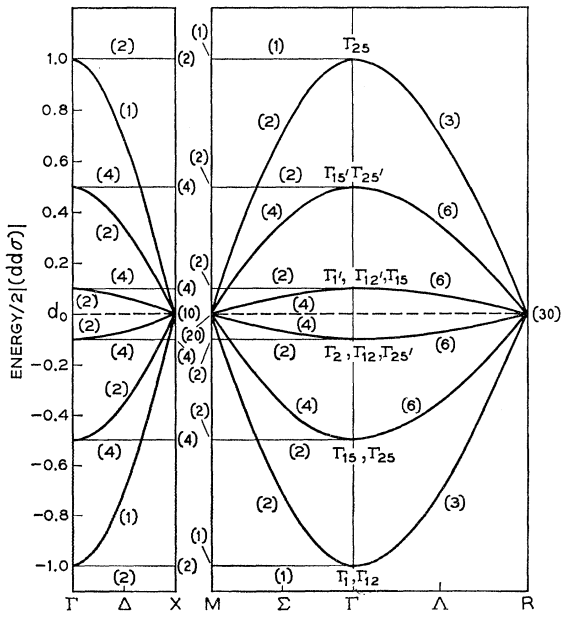

FIG. 9. $E(\mathbf{k})$ for the V atom d bands along the symmetry directions Δ, Σ, and Λ in the tight-binding, two-center, nearest-neighbor approximation.

Nevertheless, this linear-chain model does suggest reasonable explanations for some features of the APW results shown in Figs. 4 and 5. For instance, the fact that the $3d$ bandwidth is smaller at R than at other points in the Brillouin zone is probably due to the fact that this splitting results from a combination of crystalline-field effects and second- or higher-neighbor interactions. Similarly, a simple extension of this tight-binding analysis suggests a reasonable explanation for the occurrence of rather narrow X atom s and p bands in these compounds. These narrow bands cannot be attributed entirely to the relatively large separation between the X atoms in the β-wolfram structure since calculations on body-centered gallium, using the lattice constant for V_3Ga, predict nearly free-electron bands. If the 30×30 Hamiltonian matrix for the V atom d bands is augmented by the 6×6 and 2×2 matrices for the X atom s and p bands, then with the inclusion of nearest-neighbor interactions, the s and p bands remain sixfold and twofold degenerate. The introduction of second-neighbor interactions produces off-diagonal matrix elements connecting the $3d$ band states with the X atom s and p bands, so this degeneracy is presumably removed. Third-neighbor interactions are between V atom d states. Direct interactions between X atom s and p electrons result from fourth-neighbor interactions, which presumably are not large enough to broaden these bands appreciably.

It has been possible to establish contact between the APW results and those predicted by the linear chain model by means of the calculations on hypothetical V_3, which have been described in the previous section. In these calculations, the X atoms have been omitted from the β-wolfram structure and the constant potential outside the APW spheres has been varied. The results are shown in Fig. 6. Additional calculations where the constant potential outside the APW spheres has been raised another 0.39 Ry yield results at Γ which are in good agreement with those predicted by the linear-chain model. However, the d bandwidth at R is still appreciable, being approximately one-quarter the total bandwidth of 0.2 Ry found at the other symmetry points in the Brillouin zone.

V. DISCUSSION OF THE RESULTS

The current body of experimental results for these β-wolfram compounds is limited to Knight shift, susceptibility, specific heat, and superconducting transition temperature measurements. The data on super-

conducting transition temperatures is by far the most extensive and will be considered first.

The effects of band structure on the superconducting properties of elements and compounds have not yet been settled. Matthias[23] has discovered empirical rules for predicting the occurrence of superconductivity in elements, alloys, and compounds. According to these rules, the transition temperature of a given material depends critically on the average number of valence electrons per atom. In the case of the transition metals and their alloys, the high-superconducting transition temperatures are found to exist in systems containing either 5 or 7 valence electrons per atom. A plot of measured transition temperatures as a function of the average number of valence electrons per atom yields sharp maxima at 5 and 7 valence electrons per atom.

Pines[24] has attempted to interpret these empirical rules in terms of the Bardeen, Cooper, Schrieffer (BCS)[25] theory of superconductivity. Using the approximate BCS relationship between the transition temperature, T_c and the density of states at the Fermi surface $N(0)$,

$$kT_c = 1.14\langle \hbar w \rangle_{\mathrm{av}} \exp[-1/N(0)V], \qquad (3)$$

Pines concluded that the interaction parameter, V was essentially constant for the transition metals. He suggested that variations in the transition temperature as a function of the average number of valence electrons per atom were due to structure in the density-of-states curve. Recently, Morin and Maita have shown that if Eq. (3) is simplified by assuming that $\langle \hbar w \rangle_{\mathrm{av}}$ (the average energy of phonons which scatter electrons at the Fermi energy) is proportional to the Debye temperature θ_D,[26] then

$$T_c \approx \theta_D \exp[-1/N(0)V]. \qquad (4)$$

Using measured values of T_c, θ_D, and $N(0)$, they have shown that the interaction parameter, V is roughly constant over a wide range of materials. Since θ_D is found to be rather constant, this implies that the superconducting transition temperature is controlled to a large extent by the density of states at the Fermi surface. Other experiments on transition metal alloy systems include cases where the assumption of a constant interaction parameter V is justified as well as cases where it is not.[27] As a result, the accuracy of either Eq. (3) or (4) and the assumption of a constant interaction parameter is still uncertain.

Roberts[28] has made a rather comprehensive study of the correlation which exists between superconducting transition temperatures for these A_3B compounds and their mean atomic volume, electron density, and average number of valence electrons per atom. Included in this survey are the results of alloying experiments in which various atoms have been substituted into either the A or B atom sites. The most interesting result of this study is a plot of superconducting transition temperatures as a function of the average number of valence electrons per atom. This plot reveals a large number of high-temperature superconductors for materials with 4.5 to 5.0 valence electrons per atom. There are indications of a second peak centered at 6.5 valence electrons per atom, though the data for this second peak is much more limited.

If it is assumed that the transition temperatures for these A_3B compounds are determined mainly by the density of states at the Fermi surface, then it is possible to interpret this correlation between high-superconducting transition temperatures and the average valence electron number per atom ratio in terms of these APW calculations. First, it is necessary to point out that the transition temperature maxima at 4.7 and 6.5 valence electrons per atom are due to A_3B compounds having nontransition and transition element B atoms, respectively. According to the present results, the energy bands (and therefore the density of states) for these two types of A_3B compounds differ significantly, so these two peaks should be analyzed separately.

In the case of A_3B compounds having nontransition B atoms, the results of Fig. 5 suggest that a rigid-band model is appropriate. For those compounds where the A atom contains partially filled $4d$ or $5d$ bands, the d bandwidth is expected to increase somewhat, but the relative distribution of levels is expected to remain essentially unchanged. Assuming such a rigid-band model, the tendency toward high-superconducting transition temperatures for systems containing 4.5 to 5.0 valence electrons per atom correlates well with the peak in the density of states at 0.1 Ry, as shown in Fig. 8. The Fermi energies for systems containing 36 to 38 electrons per unit cell coincide with this peak in the density of states. These values are equivalent to 4.5 and 4.75 valence electrons per atom, respectively, in good agreement with the experimental transition temperature data.

For those A_3B compounds having transition element B atoms, the assumption of a rigid-band model is less certain due to strong interactions between the overlapping B and A atom d bands. The increased number of valence electrons per atom for these compounds results from the B atom d electrons. Thus, the second peak in the transition temperature at 6.5 valence

[23] B. T. Matthias, *Progress in Low Temperature Physics* (Interscience Publishers, Inc., New York, 1957), Vol. II.
[24] D. Pines, Phys. Rev. **109**, 280 (1958).
[25] J. Bardeen, L. N. Cooper, and J. R. Schrieffer, Phys. Rev. **108**, 1175 (1957).
[26] P. Morel, J. Phys. Chem. Solids **10**, 277 (1959).
[27] See for instance the proceedings of the International Conference on the Science of Superconductivity as published in Rev. Mod. Phys. **36**, 134–168 (1964). Also, *Proceedings of the Eighth International Conference on Low Temperature Physics* (Butterworths Scientific Publishers, Inc. Washington, 1963), p. 135–167.
[28] B. W. Roberts, General Electric Research Laboratories Report No. 64-RL-3540M, January 1964 (unpublished), and *Intermetallic Compounds*, edited by J. H. Westbrook (John Wiley & Sons, Inc., New York, to be published).

electrons per atom is probably due to the combined density of states which results from the overlapping B and A atom d bands. An interesting consequence of this distinction between compounds containing transition and nontransition B atoms concerns those compounds with gold B atoms. Although the gold $5d$ bands are occupied, they undoubtedly overlap the corresponding A atom d bands. Therefore, it is reasonable to expect that gold should be considered a transition metal in these compounds, with a valence of 11 rather than 1. Roberts has found that the data for the gold compounds is more consistent with the other results when a valence of 11 is assumed. Matthias[29] has arrived at a similar conclusion in connection with other gold compounds.

More direct information concerning the energy-band structure for these β-wolfram compounds has been extracted from the Knight shift and susceptibility data by Clogston, Jaccarino, and co-workers.[2,6] Blumberg *et al.*,[4] observed a correlation between the temperature dependence of the Knight shift and the superconducting transition temperatures for a number of these β-wolfram compounds. Those compounds with high-superconducting transition temperatures exhibited strongly temperature-dependent Knight shifts. Williams and Sherwood[5] observed a similar correlation in the susceptibility. On the basis of these results, Clogston and Jaccarino have proposed an energy-band model for V_3Ga. A striking feature of this model is that it predicts a high, narrow peak in the density of states at the Fermi energy for V_3Ga. Subsequent measurements of the electronic specific heat by Morin and Maita[3] yielded a very large value for γ (the coefficient of T in the power-series expansion of the heat capacity), a result which is consistent with the Clogston-Jaccarino model.

Clogston, Jaccarino, and co-workers have interpreted the Knight shift and susceptibility data for V_3Ga in terms of this simplified energy-band model.[2,6] Using atomic estimates of the hyperfine fields due to unpaired vanadium $3d$ and gallium $4p$ electrons at the Fermi surface, they find that approximately equal fractions of vanadium $3d$ and gallium $4p$ wave-function character are required at the Fermi surface to explain the Knight shift data in terms of a core-polarization mechanism. A limited sampling of the APW wave functions in the vicinity of the Fermi energy indicates a rather small admixture of gallium $4p$-type character, amounting to approximately 5%. This result has been found to be insensitive to reasonable variations in the vanadium and gallium potentials, the gallium APW sphere radius, etc. This discrepancy is at present not understood.

One difficulty with the rigid-band model for these V_3X compounds having nontransition X atoms concerns the differences in the density of states at the Fermi surface $N(0)$ for V_3Si and V_3Ge, respectively. From the low-temperature specific heat measurements, Morin and Maita obtain values for $N(0)$ of 5.5 and 2.14 spin states per eV-vanadium atom for V_3Si and V_3Ge, respectively. These values are considerably larger than the value of 1.3 spin states per eV vanadium atom that has been obtained from the crude density-of-states calculation described in Sec. III. If a rigid-band model is valid, these differences must be due either to fine structure in the density of states which is beyond the accuracy of the present calculations or to phonon enhancement of the specific-heat density of states, as Clogston has suggested.[11]

Clearly, the experimental results for these β-wolfram compounds are rather limited so that the accuracy of the present calculations remains somewhat uncertain. In view of the complicated nature of the calculated energy bands, it is encouraging to find at least qualitative agreement between the Clogston-Jaccarino model and the APW results. Hopefully, the results of these calculations will stimulate additional experiments on these compounds that will elucidate their band structure more precisely.

ACKNOWLEDGMENTS

It is a pleasure to thank A. M. Clogston, not only for originally suggesting this study, but also for many useful discussions and valuable suggestions during the entire course of this work. The author is grateful to A. C. Switendick for providing copies of his APW programs and for his generous assistance and advice in adapting these programs to the β-wolfram structure. The author has benefitted from numerous discussions with J. H. Wood, R. E. Watson, J. C. Phillips, J. H. Wernick, V. Jaccarino, and Y. Yafet on various aspects of this problem.

[29] B. T. Matthias, J. Phys. Chem. Solids **10**, 342 (1959).